CO2 trapping in amorphous H2O ice: Relevance to polar mesospheric cloud particles

ARTICLE *in* JOURNAL OF ATMOSPHERIC AND SOLAR-TERRESTRIAL PHYSICS · MARCH 2015

Impact Factor: 1.47 · DOI: 10.1016/j.jastp.2015.03.004

3 AUTHORS:

Thomas Mangan
University of Leeds
1 PUBLICATION **1** CITATION
SEE PROFILE

Victoria L. Frankland
University of Leeds
12 PUBLICATIONS **4** CITATIONS
SEE PROFILE

John M. C. Plane
University of Leeds
420 PUBLICATIONS **8,127** CITATIONS
SEE PROFILE

Journal of Atmospheric and Solar-Terrestrial Physics ∎ (∎∎∎∎) ∎∎∎–∎∎∎

Contents lists available at ScienceDirect

Journal of Atmospheric and Solar-Terrestrial Physics

journal homepage: www.elsevier.com/locate/jastp

ATP4040: CO_2 trapping in amorphous H_2O ice: Relevance to polar mesospheric cloud particles

T.P. Mangan, V.L. Frankland, J.M.C. Plane *

School of Chemistry, University of Leeds, Leeds LS2 9JT, UK

ARTICLE INFO

Article history:
Received 16 October 2014
Received in revised form
5 March 2015
Accepted 6 March 2015

Keywords:
Amorphous ice
Carbon dioxide trapping
Temperature programmed desorption
Polar mesospheric clouds

ABSTRACT

Polar mesospheric clouds form in the summer high latitude mesopause region and are primarily comprised of H_2O ice, forming at temperatures below 150 K. Average summertime temperatures in the polar mesosphere (78°N) are approximately 125 K and can be driven lower than 100 K by gravity waves. Under these extreme temperature conditions and given the relative mesospheric concentrations of CO_2 and H_2O ($\sim$360 ppmv and $\sim$10 ppmv, respectively) it has been hypothesised that CO_2 molecules could become trapped within amorphous mesospheric ice particles, possibly making a significant contribution to the total condensed volume. Studies of CO_2 trapping in co-deposited gas mixtures of increasing CO_2:H_2O ratio (deposited at 98 K) were analysed *via* temperature programmed desorption. CO_2 trapping was found to be negligible when the H_2O flux to the surface was reduced to 4.8×10^{13} molecules cm^{-2} s^{-1}. This corresponds to an average of 0.4 H_2O molecules depositing on an adsorbed CO_2 molecule and thereby trapping it in amorphous ice. Extrapolating the experimental data to mesospheric conditions shows that a mesospheric temperature of 100 K would be required (at a maximum mesospheric H_2O concentration of 10 ppmv) in order to trap CO_2 in the ice particles. Given the rarity of this temperature being reached in the mesosphere, this process would be an unlikely occurrence.

1. Introduction

Polar mesospheric clouds (PMCs) (also known as noctilucent clouds) are optically thin clouds that form in the summer polar mesopause region. PMCs primarily consist of small H_2O ice particles with median radii of $\sim$51 nm (von Cossart et al., 1999; Hervig et al., 2001), which can form when the temperature falls below the water frost point (150 K). Larger ice particles which sediment to the bottom of the ice layer, at altitudes between 82 and 85 km, scatter sufficient light to become optically visible (Rapp and Thomas, 2006).

A major source of ice nuclei for heterogeneous nucleation in the mesosphere are meteoric smoke particles (MSPs) (Rapp and Thomas, 2006; Plane, 2011). MSPs are a product of ablation and subsequent recondensation of meteoric material (Saunders and Plane, 2006), of which somewhere between 10 and 110 tonnes enters the atmosphere daily (Plane, 2012). Average temperatures in the high latitude upper mesosphere (78°N) during summertime are approximately 125 K, while gravity waves can drive temperatures lower than 100 K (Lübken et al., 2009). Murray and Jensen (2010) showed that homogeneous nucleation may also be possible under extreme mesospheric temperature conditions below 110 K. These authors also suggested that amorphous ice may preferentially nucleate due to a lower energy barrier to nucleation compared to crystalline ice. Satellite measurements indicate PMCs are composed primarily of crystalline ice but could not rule out amorphous ice formation (Hervig and Gordley, 2010).

H_2O is present in the high latitude mesopause during the summertime at concentrations of up to 10 ppmv (Rong et al., 2010). The source of H_2O vapour in the mesosphere is due to a combination of atmospheric upwelling and methane oxidation via reaction with $O(^1D)$ and OH radicals (Thomas, 1991). CO_2 is well mixed vertically with concentrations $>$360 ppmv up to altitudes of approximately 80 km, above which UV photolysis of CO_2 (to CO and O) and gravitational separation with respect to lighter gas species become dominant removal processes. Due to increasing anthropogenic sources of CO_2, a global decadal increase of 23.5 ± 6.3 ppmv is currently observed (Emmert et al., 2012). Given the concentrations of trace species present in the mesosphere during the PMC cloud season and the extreme low temperatures, it is possible that CO_2 trapping in amorphous solid water (ASW) ice could be a viable process. However, it should be noted CO_2 cannot become trapped when ASW has irreversibly crystallised to crystalline solid water (CSW) ice, or when ice is initially deposited as CSW ice.

CO_2 trapping in ASW ice has been experimentally observed

* Corresponding author.
E-mail address: j.m.c.plane@leeds.ac.uk (J.M.C. Plane).

http://dx.doi.org/10.1016/j.jastp.2015.03.004
1364-6826/

under conditions relevant to the interstellar medium (ISM) (Galvez et al., 2007; Malyk et al., 2007; Mate et al., 2008). However, these studies looked at deposition temperatures below atmospheric relevance (≤ 90 K) and low CO_2:H_2O ratios ($\sim 0.02{:}1$ to $0.7{:}1$) due to the composition of interstellar ice. Experimental studies have also investigated CO_2 trapping in the Martian regolith (Trainer et al., 2010), but these were at higher temperatures and pressures than those observed during the PMC cloud season. To our knowledge, studies of co-deposition of high CO_2:H_2O ratio gas mixtures at conditions relevant to the Earth's mesosphere have not been performed. In the present study, the co-deposition of high CO_2:H_2O ratio mixtures were studied using temperature programmed desorption (TPD) to determine the mesospheric conditions under which CO_2 trapping in ASW ice would be possible. The experimental procedure is described in Section 2, and the results and discussion in Section 3.

2. Experimental procedure

The experiments were undertaken in an ultra-high vacuum (UHV) chamber with an internal volume of ~ 25 L (see Fig. 1). This system has been previously described by Vondrak et al. (2006). Briefly, the chamber is pumped *via* a 550 L s^{-1} turbo-molecular pump (Varian Turbo-V 551 Navigator) backed by a rotary pump (Varian, DS302), achieving a base pressure of typically $< 7 \times 10^{-10}$ mbar. The chamber is equipped with a quadrupole mass spectrometer (QMS) (Hiden, HAL 3F 301 RC PIC), a needle valve (NUPRO, SS4BK) for gas dosing and an inert ion (Ar^+) sputter source (PSP technology Ltd., ISIS 3000) which was modified to function as a leak valve for this study. Within the centre of the UHV chamber is a cylindrical Cu (111) crystal sample of 12 mm diameter and 2.5 mm thickness, polished to 1 μm and oriented to $\pm 0.5°$ of the (111) plane. The crystal is mounted *via* tungsten (W) heating wires onto an oxygen free high conductivity (OFHC) cold finger (shown in Fig. 1), which in turn is mounted onto an xyzθ manipulator. The sample is liquid nitrogen cooled to a base temperature of approximately 98 K and can be heated resistively by the W wires embedded in the perimeter of the Cu (111) crystal. The surface temperature is monitored using a K-type thermocouple positioned in a small hole on the side of the Cu (111) crystal. Prior to each experiment the Cu (111) crystal was annealed to 800 K for 30 min.

H_2O (deionised) was subject to three freeze-pump-thaw cycles and CO_2 (from dry ice) was first purified by pumping. CO_2:H_2O gas mixtures at ratios varying from 1:1 to 13:1 were prepared using manometric techniques on a glass gas-handling line, and then dosed onto the Cu (111) crystal *via* the needle valve in the form of a collimated effusive beam. This beam has a diameter only slightly larger than the Cu (111) crystal and therefore minimises adsorption (and therefore desorption) of either species onto other nearby surfaces such as the OFHC cold finger (see Fig. 1). Any species adsorbed onto the W wires would desorb immediately upon heating. The dosing rates were calibrated for CO_2 and H_2O separately through beam flux calibrations based on the procedure of Oakes (1994). Briefly, the beam flux (F_{beam}) is calculated from the exponential decay of a gas species from the point where the input gas flow has been terminated. The exponential decay is described by:

$$P = P_0 \exp^{-Cmt} \tag{1}$$

where P is the pressure, P_0 is the initial pressure at the termination of the dose, C_m is the pumping coefficient for the gas and t is the time from the start of the decay. Eq. (1) was linearised and C_m obtained from the gradient. From this F_{beam} is given by:

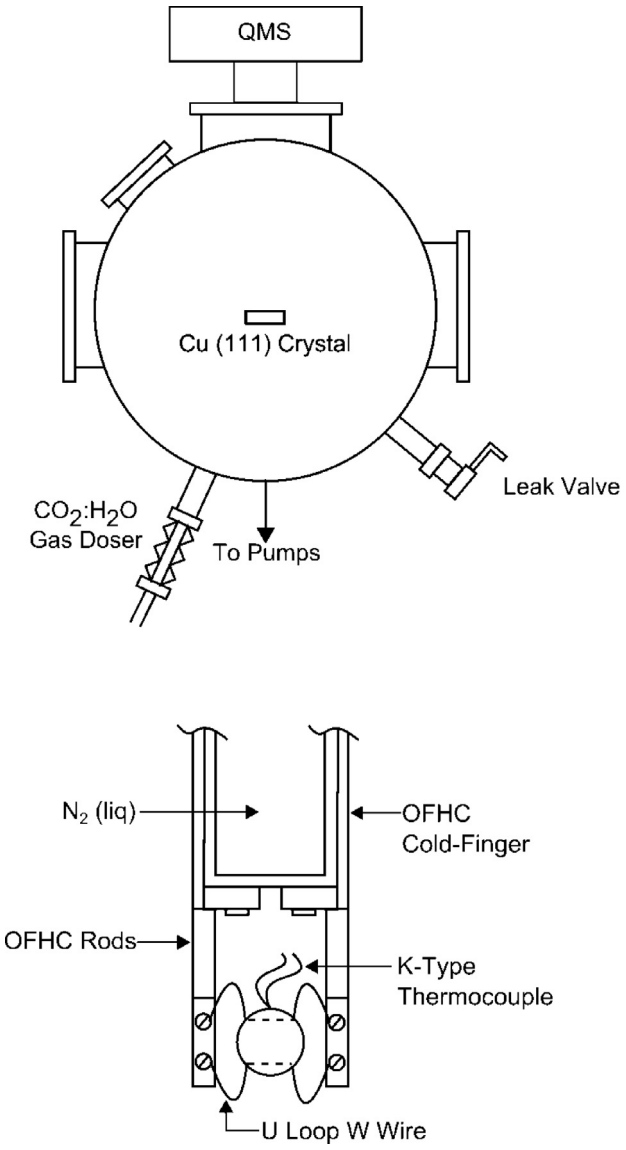

Fig. 1. Schematic diagram of the UHV chamber upper level (top) and Cu (111) crystal mount (bottom).

$$F_{beam} = \frac{V_{system} C_m P_0}{k_B T A_{beam}} \tag{2}$$

where V_{system} is the volume of the chamber, k_B is the Boltzmann constant, T the temperature of the gaseous species and A_{beam} the cross sectional area of the molecular beam. The CO_2 and H_2O fluxes varied from $(3.4 - 6.3) \times 10^{14}$ molecules cm^{-2} s^{-1} and $(0.5–3.4) \times 10^{14}$ molecules cm^{-2} s^{-1}, respectively. The total flux of CO_2 and H_2O remained the same (within experimental error) for all the experiments (6.8×10^{14} molecules cm^{-2} s^{-1}).

In a typical experiment, the gas mixture was dosed for 7200 s onto the Cu (111) crystal at a base temperature of 98 K. This enabled the H_2O film to form as ASW ice. The absorbed species were then analysed *via* TPD, where the Cu crystal was heated between 98 and 200 K at a heating ramp of 0.25 K s^{-1}. This ensured that all dosed species had desorbed. The CO_2 TPD profiles described in the following section were corrected against a pure CO_2 TPD trace to remove the surface CO_2 desorption. This surface CO_2 is weakly physisorbed to the ASW ice surface and rapidly desorbs upon sample heating, peaking at temperatures of approximately 125 K, which is more than 20 K lower than the observed initial

Please cite this article as: Mangan, T.P., et al., ATP4040: CO_2 trapping in amorphous H_2O ice: Relevance to polar mesospheric cloud particles. Journal of Atmospheric and Solar-Terrestrial Physics (2015), http://dx.doi.org/10.1016/j.jastp.2015.03.004

desorption of trapped CO_2.

3. Results and discussion

The background corrected CO_2 TPD traces are shown in Fig. 2 and display only the desorption features of CO_2 trapped within the water ice matrix. The first desorption feature prominently occurring in the 1:1 and 3:1 CO_2:H_2O ratio experiments appears at approximately 157 K and is known as a molecular volcano peak (Smith et al., 1997). The other CO_2 desorption feature (co-desorption peak) appears between 165–175 K and is more prominent at higher ratios compared to the molecular volcano peak. As the CO_2:H_2O ratio in the dosing mixture is increased (and thus the H_2O flux decreased), the molecular volcano peak becomes less prominent, followed by a reduction in the co-desorption peak until no CO_2 desorption features were observed. Therefore the 13:1 CO_2:H_2O ratio was determined as the point where no CO_2 desorption occurred from the ice matrix in this study. This observation of the CO_2 desorption features reducing with respect to increasing CO_2:H_2O ratio is consistent with the findings of Galvez et al. (2008).

The CO_2 trapping processes can be explained by comparing the CO_2 TPD traces with their corresponding H_2O TPD trace (Fig. 3). Each H_2O TPD trace contains two peaks: an ASW desorption peak; followed by the desorption feature for CSW at a higher temperature. The H_2O ice layers were of sufficient thickness (125–880 nm) for the CSW peak to be observed at all CO_2:H_2O ratios. The ASW desorption peak occurs at approximately the same temperature as the corresponding CO_2 molecular volcano peak. As the H_2O film thickness increases the ASW peak (and therefore the CO_2 molecular volcano) shift to higher temperatures. The CSW desorption peak also coincides with the CO_2 co-desorption peak. These peaks also shift to higher temperatures with increasing H_2O film thickness. Both of these observations in our co-deposited ice are consistent with previous studies of trapped species in layered ASW ice films deposited at ~25 K (May et al., 2012, 2013). Deposition of ASW at 98 K leads to a less porous and thus higher density (~0.8 g cm^3) form of ASW ice than at lower temperatures (Brown et al., 1996). However, as the ices in this study were co-deposited, the difference in the nature of the ASW ice formed does not affect the CO_2 trapping results here as they would in layered systems.

The release of trapped CO_2 (molecular volcano feature) from the ASW ice matrix can be explained using one of two theories: the glass transition; and crystallisation-induced cracking. In the first theory, the ASW film undergoes a glass transition during annealing (Jenniskens and Blake, 1994) which transforms the film into a viscous liquid enabling the H_2O molecules to re-organise and freeze into the crystalline phase (CSW ice). This molecular reorganisation causes cavities in the ice matrix to open, releasing

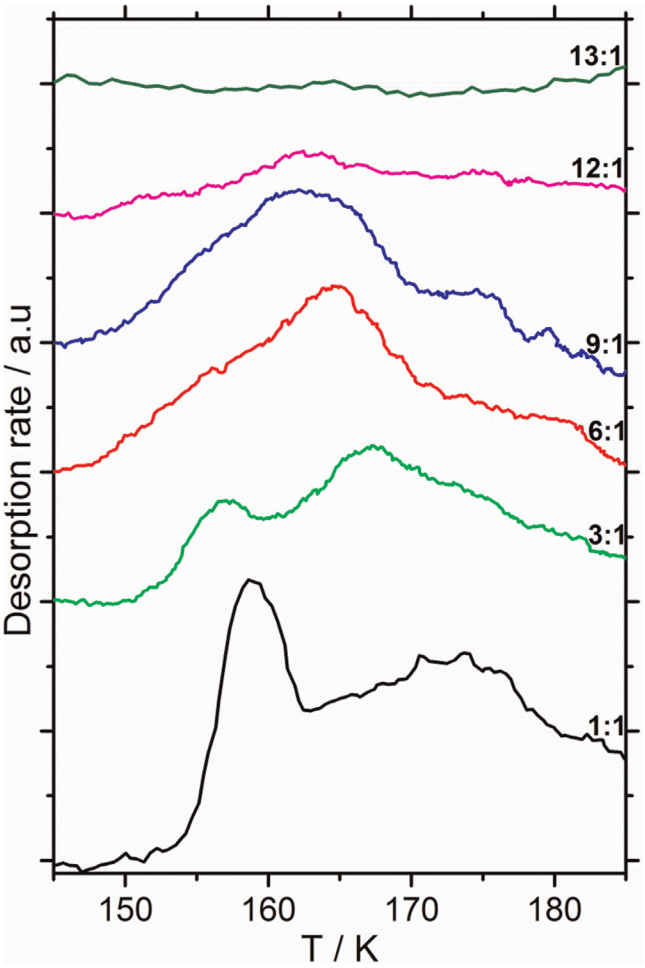

Fig. 2. CO_2 background corrected TPD traces showing the desorption rate (arbitrary units) against temperature for trapped CO_2/ice films (offset for clarity; the zero in each plot is the value at 145 K). The CO_2:H_2O ratio in the dosing mixture is indicated on the right-hand side of each plot.

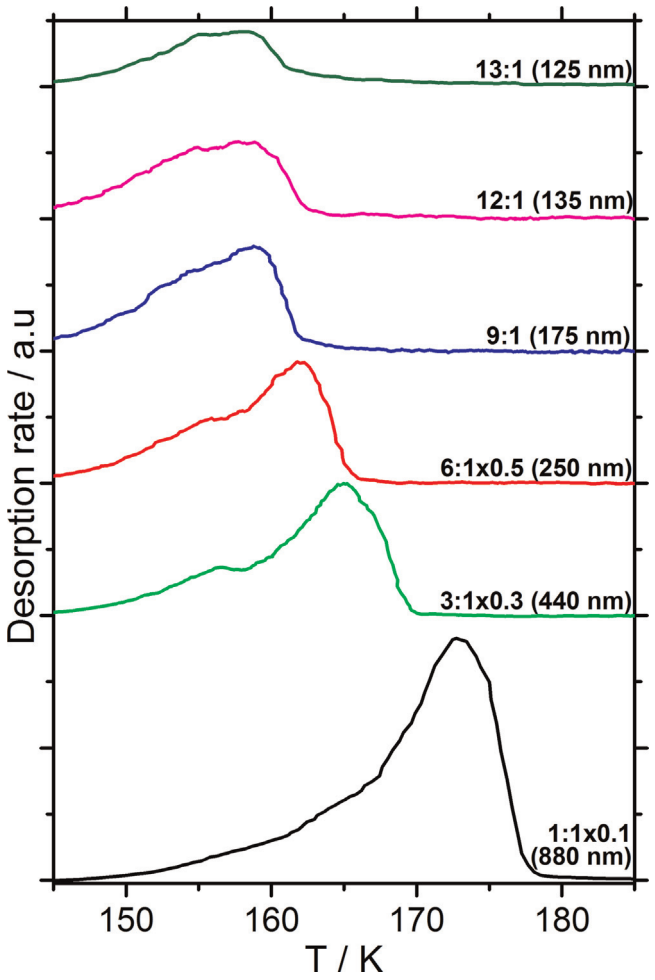

Fig. 3. H_2O TPD traces showing the desorption rate (arbitrary units) against temperature for the same CO_2:H_2O ratios as in Fig. 2 (note that the traces are offset for clarity). Each H_2O trace is labelled with the CO_2:H_2O ratio, the factor by the data has been rescaled for clarity (if applied) and, in parenthesis, the estimated film thickness in nm.

Please cite this article as: Mangan, T.P., et al., ATP4040: CO_2 trapping in amorphous H_2O ice: Relevance to polar mesospheric cloud particles. Journal of Atmospheric and Solar-Terrestrial Physics (2015), http://dx.doi.org/10.1016/j.jastp.2015.03.004

the trapped CO_2 molecules (as a molecular volcano) in the uppermost part of the H_2O film. The temperature of this H_2O glass transition is dependant on several variables including the initial deposition temperature and the heating rate applied (Jenniskens and Blake, 1996). The end of the glass transition can be observed in H_2O TPDs as a reduction in ASW desorption rate as crystallisation to CSW dominates, before CSW desorbs. In the second more recent theory, the H_2O ice remains in the solid phase throughout the ASW to CSW transition. During crystallisation, cracks propagate down through the H_2O film enabling the CO_2 trapped in cavities to escape to vacuum (May et al., 2012, 2013). This theory is better able to explain the shift to higher temperatures in the CO_2 molecular volcano with respect to increasing film thickness (May et al., 2011), as observed in the present study. However, regardless of whether the ASW to CSW phase transition remains in the solid phase or temporarily transforms into a viscous liquid does not affect the conclusions of the present study regarding the mesospheric significance of CO_2 trapping.

The CO_2 co-desorption peak appears at the temperature where maximum desorption of CSW occurs. This corresponds to the release of the remaining CO_2 trapped in the lower layers of the ice matrix that did not have access to the outer surface of the H_2O film during crystallisation (Kumi et al., 2006; Malyk et al., 2007).

As the CO_2 flux increases with increasing CO_2:H_2O ratio, CO_2 trapping is limited by the reduction in the H_2O flux until no CO_2 desorption features from the water ice matrix were observed (13:1 CO_2:H_2O ratio). Experimentally, this corresponds to a lower limit H_2O flux of 4.8×10^{13} molecules $cm^{-2}\,s^{-1}$. H_2O fluxes below this value are therefore not high enough to close micro-pores at the ASW surface before CO_2 molecules desorb during dosing (Galvez et al., 2008).

Using the experimental value for the H_2O flux lower limit (required for CO_2 trapping in ASW) a comparison to a realistic value of H_2O flux in the polar mesosphere can be undertaken. The mesospheric H_2O flux (in units of molecules $cm^{-2}\,s^{-1}$) is given by:

$$H_2O\ \text{flux} = \frac{\bar{c}}{4}[H_2O] \tag{3}$$

where $\bar{c}$ is the mean thermal velocity of the H_2O molecules (in units of $cm\,s^{-1}$) and is given by:

$$\bar{c} = 1.46 \times 10^4 \sqrt{T/M} \tag{4}$$

where T is the absolute temperature and M is the molar mass (in g). The concentration of H_2O molecules, $[H_2O]$, in the polar mesosphere was calculated assuming optimal PMC cloud season conditions (10 ppmv of H_2O at a total pressure of 1 Pa at 83 km). At a temperature of 98 K, the maximum H_2O flux would be 6.3×10^{13} molecules $cm^{-2}\,s^{-1}$, which is higher than the experimental threshold determined in this study (4.8×10^{13} molecules $cm^{-2}\,s^{-1}$). A mesospheric CO_2 flux of 1.2×10^{15} molecules $cm^{-2}\,s^{-1}$ (360 ppmv of CO_2 at a total pressure of 1 Pa at 83 km) can be estimated in the same way. This is higher than the experimental CO_2 flux range used in this study ($(3.4–6.3) \times 10^{14}$ molecules $cm^{-2}\,s^{-1}$) indicating that sufficient CO_2 would be available in the mesosphere. However, this is at a temperature of 98 K, which is very rarely encountered (Lübken et al., 2009). Furthermore, H_2O would have likely condensed, either via heterogeneous (Rapp and Thomas, 2006; Plane, 2011) or homogeneous (Murray and Jensen, 2010) nucleation, to form pure ice particles well before such a low temperature was reached.

In order to determine the complete range of conditions that would be required in the mesosphere to trap CO_2, it is necessary to estimate the average number of H_2O molecules depositing onto an already adsorbed CO_2 molecule, in order to prevent it desorbing. First, the residence time of an adsorbed CO_2 on the ASW surface, τ,

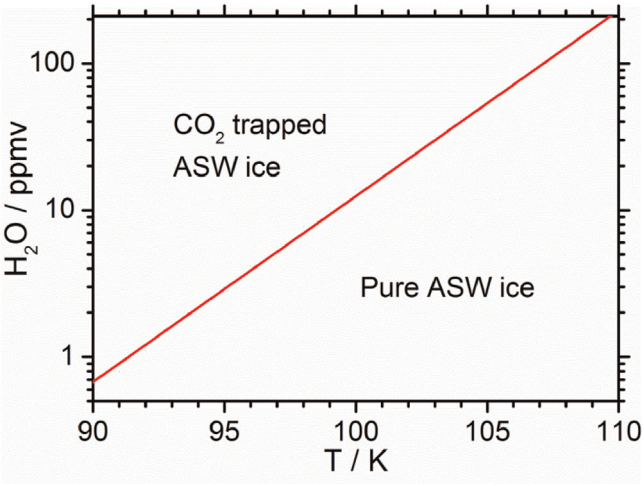

Fig. 4. A plot of the minimum H_2O concentration (ppmv) required to trap CO_2 in ASW, as a function of temperature (K).

is the reciprocal of the desorption rate coefficient, k_{des}, which is given by Attard (1998) as:

$$\tau = \frac{1}{k_{des}} = \frac{1}{A \exp\left(-E_{des}/RT\right)} \tag{5}$$

where the pre-exponential factor A is the frequency of oscillation corresponding to the average of the librational modes of CO_2 ($2.9 \times 10^{12}\,s^{-1}$) and E_{des} is the binding energy of CO_2 on ASW ($23.7\,kJ\,mol^{-1}$), which have been measured by Sandford and Allamandola (1990). The CO_2 surface residence time at 98 K is $\tau = 1.48$ s. Taking the collision cross section of a CO_2 molecule as $0.52\,nm^2$ (Atkins and De Paula, 2002) and the measured lower limit of the H_2O flux (4.8×10^{13} molecules $cm^{-2}\,s^{-1}$), a minimum of 0.4 H_2O molecules must deposit on an adsorbed CO_2 molecule in order to trap it in the amorphous ice.

This result can now be used to determine the minimum H_2O mixing ratio (in units of ppmv) required for CO_2 trapping in ASW across a range of temperatures in the upper mesosphere, as shown in Fig. 4. The region above the line indicates plausible conditions for CO_2 trapping in ASW. The current maximum mesospheric H_2O concentration typical of the PMC cloud season is 10 ppmv (Rong and Russell, 2010), which implies that a temperature below 100 K would be required for CO_2 trapping within PMC ice particles. At higher temperatures ($\sim$110 K) the H_2O concentration would need to be over an order of magnitude higher for CO_2 trapping to become a significant process.

Acknowledgements

This work was supported by the European Research Council (Project number 291332- CODITA), and a PhD studentship for TPM from the UK Natural Environment Research Council.

References

Atkins, P.W., De Paula, J., 2002. Atkins' Physical Chemistry. Oxford University Press, Oxford.

Attard, G.B.C., 1998. Surfaces. Oxford University Press, Oxford.

Brown, D.E., George, S.M., Huang, C., Wong, E.K.L., Rider, K.B., Smith, R.S., Kay, B.D., 1996. H_2O condensation coefficient and refractive index for vapor-deposited ice from molecular beam and optical interference measurements. J. Phys. Chem. 100 (12), 4988–4995.

Emmert, J.T., Stevens, M.H., Bernath, P.F., Drob, D.P., Boone, C.D., 2012. Observations of increasing carbon dioxide concentration in Earth's thermosphere. Nat.

Geosci. 5 (12), 868–871.
Galvez, O., Mate, B., Herrero, V.J., Escribano, R., 2008. Trapping and adsorption of CO_2 in amorphous ice: a FTIR study. Icarus 197 (2), 599–605.
Galvez, O., Ortega, I.K., Mate, B., Moreno, M.A., Martin-Llorente, B., Herrero, V.J., Escribano, R., Gutierrez, P.J., 2007. A study of the interaction of CO_2 with water ice. Astron. Astrophys. 472 (2), 691–698.
Hervig, M.E., Gordley, L.L., 2010. Temperature, shape, and phase of mesospheric ice from solar occultation for ice experiment observations. J. Geophys. Res. 115, article no.: D15208.
Hervig, M.E., Thompson, R.E., McHugh, M., Gordley, L.L., Russell, J.M., Summers, M. E., 2001. First confirmation that water ice is the primary component of polar mesospheric clouds. Geophys. Res. Lett. 28 (6), 971–974.
Jenniskens, P., Blake, D.F., 1994. Structural transitions in amorphous water ice and astrophysical implications. Science 265 (5173), 753–756.
Jenniskens, P., Blake, D.F., 1996. Crystallization of amorphous water ice in the solar system. Astrophys. J. 473 (2), 1104–1113.
Kumi, G., Malyk, S., Hawkins, S., Reisler, H., Wittig, C., 2006. Amorphous solid water films: transport and guest-host interactions with CO_2 and N_2O dopants. J. Phys. Chem. A 110 (6), 2097–2105.
Lübken, F.J., Lautenbach, J., Hoffner, J., Rapp, M., Zecha, M., 2009. First continuous temperature measurements within polar mesosphere summer echoes. J. Atmos. Sol.-Terr. Phys. 71 (3–4), 453–463.
Malyk, S., Kumi, G., Reisler, H., Wittig, C., 2007. Trapping and release of CO_2 guest molecules by amorphous ice. J. Phys. Chem. A 111 (51), 13365–13370.
Mate, B., Galvez, O., Martin-Llorente, B., Moreno, M.A., Herrero, V.J., Escribano, R., Artacho, E., 2008. Ices of CO_2/H_2O mixtures. Reflection-absorption IR spectroscopy and theoretical calculations. J. Phys. Chem. A 112 (3), 457–465.
May, R.A., Smith, R.S., Kay, B.D., 2011. Probing the interaction of amorphous solid water on a hydrophobic surface: dewetting and crystallization kinetics of ASW on carbon tetrachloride. Phys. Chem. Chem. Phys. 13 (44), 19848–19855.
May, R.A., Smith, R.S., Kay, B.D., 2012. The molecular volcano revisited: determination of crack propagation and distribution during the crystallization of nanoscale amorphous solid water films. J. Phys. Chem. Lett. 3 (3), 327–331.
May, R.A., Smith, R.S., Kay, B.D., 2013. The release of trapped gases from amorphous solid water films. I. "Top-down" crystallization-induced crack propagation probed using the molecular volcano. J. Chem. Phys. 138 (10), 104501.
May, R.A., Smith, R.S., Kay, B.D., 2013. The release of trapped gases from amorphous solid water films. II. "Bottom-up" induced desorption pathways. J. Chem. Phys. 138, 10.
Murray, B.J., Jensen, E.J., 2010. Homogeneous nucleation of amorphous solid water particles in the upper mesosphere. J. Atmos. Sol.-Terr. Phys. 72 (1), 51–61.
Oakes, D.J., 1994. Dissociative Adsorption of Simple Alkanes Induced by Hypertherman Collisions with Platinum. School of Chemical Sciences, University of East Anglia, Norwich, UK (Ph.D. thesis).
Plane, J.M.C., 2011. On the role of metal silicate molecules as ice nuclei. J. Atmos. Sol.-Terr. Phys. 73 (14–15), 2192–2200.
Plane, J.M.C., 2012. Cosmic dust in the earth's atmosphere. Chem. Soc. Rev. 41 (19), 6507–6518.
Rapp, M., Thomas, G.E., 2006. Modeling the microphysics of mesospheric ice particles: assessment of current capabilities and basic sensitivities. J. Atmos. Sol.-Terr. Phys. 68 (7), 715–744.
Rong, P., Russell III, J.M., Gordley, L.L., Hervig, M.E., Deaver, L., Bernath, P.F., Walker, K.A., 2010. Validation of v1.022 mesospheric water vapor observed by the Solar Occultation for Ice Experiment instrument on the Aeronomy of Ice in the Mesosphere satellite. J. Geophys. Res. 115, article no.: D24314.
Sandford, S.A., Allamandola, L.J., 1990. The physical and infrared spectral properties of CO_2 in astrophysical ice analogs. Astrophys. J. 355 (1), 357–372.
Saunders, R.W., Plane, J.M.C., 2006. A laboratory study of meteor smoke analogues: composition, optical properties and growth kinetics. J. Atmos. Sol.-Terr. Phys. 68 (18), 2182–2202.
Smith, R.S., Huang, C., Wong, E.K.L., Kay, B.D., 1997. The molecular volcano: abrupt CCl_4 desorption driven by the crystallization of amorphous solid water. Phys. Rev. Lett. 79 (5), 909–912.
Thomas, G.E., 1991. Mesospheric clouds and the physics of the mesopause region. Rev. Geophys. 29 (4), 553–575.
Trainer, M.G., Tolbert, M.A., McKay, C.P., Toon, O.B., 2010. Enhanced CO_2 trapping in water ice via atmospheric deposition with relevance to Mars. Icarus 206 (2), 707–715.
von Cossart, G., Fiedler, J., von Zahn, U., 1999. Size distributions of NLC particles as determined from 3-color observations of NLC by ground-based lidar. Geophys. Res. Lett. 26 (11), 1513–1516.
Vondrak, T., Plane, J.M.C., Meech, S.R., 2006. Influence of submonolayer sodium adsorption on the photoemission of the Cu(111)/water ice surface. J. Chem. Phys. 125 (22), article no.: 224702.

Please cite this article as: Mangan, T.P., et al., ATP4040: CO_2 trapping in amorphous H_2O ice: Relevance to polar mesospheric cloud particles. Journal of Atmospheric and Solar-Terrestrial Physics (2015), http://dx.doi.org/10.1016/j.jastp.2015.03.004